Journal of Medicinal Chemistry

Article

Tyrocidine A Analogues Bearing the Planar D-Phe-2-Abz Turn Motif: How Conformation Impacts Bioactivity

Alan J. Cameron, Patrick J.B. Edwards, Elena Harjes, and Vijayalekshmi Sarojini

J. Med. Chem., **Just Accepted Manuscript** • DOI: 10.1021/acs.jmedchem.7b00953 • Publication Date (Web): 15 Nov 2017

Just Accepted

ACS Publications

Journal of Medicinal Chemistry is published by the American Chemical Society. 1155 Sixteenth Street N.W., Washington, DC 20036

Tyrocidine A Analogues Bearing the Planar D-Phe-2-Abz Turn Motif: How Conformation Impacts Bioactivity

Alan J. Cameron[a], Patrick J. B. Edwards[b], Elena Harjes[b] and Vijayalekshmi Sarojini[a,*]

[a]School of Chemical Sciences, University of Auckland, Auckland 1142, New Zealand.

[b]Institute of Fundamental Sciences, Massey University, Palmerston North 4442, New Zealand.

*Author for correspondence

Vijayalekshmi Sarojini

Phone: + 64 9 9233387

E-mail: v.sarojini@auckland.ac.nz

Abstract

The D-Phe-Pro β-turn of the cyclic β-hairpin antimicrobial decapeptide Tyrocidine A, (Tyrc A) was substituted with the D-Phe-2-aminobenzoic acid (2-Abz) motif in a synthetic analogue (**1**). NMR structure of **1** demonstrated that compound **1** retained the β-hairpin structure of Tyrc A with additional planarity, resulting in approx. 30-fold reduced haemolysis than Tyrc A. Although antibacterial activity was partially compromised, a single Gln to Lys substitution (**2**) restored activity equivalent to Tyrc A against *S. aureus*, enhanced activity against two Gram negative strains and maintained the reduced haemloysis of **1**. Analysis by transmission electron microscopy (TEM) suggested a membrane lytic mechanism of action for these peptides. Compound **2** also exhibits nanomolar antifungal activity in synergy with amphotericin B. The D-Phe-2-Abz turn may serve as a tool for the synthesis of structurally predictable β-hairpin libraries. Unlike traditional β-turn motifs such as D-Pro-Gly, both the 2-Abz and D-Phe rings may be further functionalized.

Introduction

Tyrocidine A (Tyrc A, Figure 1) is a membrane lytic cyclic antimicrobial peptide (AMP) with low micromolar activity against Gram positive pathogens and fungi, but is largely inactive against Gram negative bacteria.[1-3] Like gramicidin S (Figure 1), Tyrc A also forms a cyclic β-sheet.[4] The X-ray crystal structure of Tyrc A reveals the presence of a type II' β-turn formed by residues Leu^{10}, D-Phe^{1}, Pro^{2} and Phe^{3} with $C^{\alpha}_{i} - C^{\alpha}_{i+3}$ distance of 5.28 Å.[5] At the other end of the molecule, a distorted type I turn is formed.[5] The molecule forms an amphipathic β-sheet with a curvature (Figure 3A) distinct from the more planar backbone of gramicidin S.[5] The

amphipathicity arises from the lower face of the molecule (concave face) containing more hydrophilic and cationic side chains, while the upper face is predominantly hydrophobic (Figure 3).[5] The crystal structure also revealed Tyrc A to occur as an amphipathic intermolecular dimer, a feature likely important in its antibacterial mode of action.[5] Tyrothricin, a mixture of tyrocidines A-D and gramicidin, was the first commercial antibiotic mixture, used under trade names Limex and Tyrosur[3-4, 6] Although this mixture is noted to have significant antibacterial, antifungal and antimalarial properties, its clinical use and that of both Tyrc A and gramicidin S is limited to topical applications due to significant haemloysis and toxicity to both liver and kidneys.[2-4, 7] Additionally, this family of peptides possess poor activity against Gram-negative bacteria.[8-9]. Overcoming these major drawbacks may pave the way towards their development as broad spectrum antimicrobials.

Unique turn conformations of 2-amino benzoic acid (2-Abz) containing peptides have previously been reported in model peptides devoid of known biological activities.[10-13] Work from our laboratory demonstrated that D-Phe-2-Abz motif adopts a unique turn conformation.[14] We wanted to explore the applications of D-Phe-2-Abz as a turn motif in the synthesis of antimicrobial peptides, the development of which is a major focus of our research.[15-16] Tyrc A, with its well characterised β-hairpin structure and antimicrobial activity, but inherent drawbacks, appeared a good candidate for these studies. The relationship between the molecular conformation and bioactivity of two novel analogues (Figure 1), employing the D-Phe-2-Abz turn motif, are presented, in comparison to Tyrc A.

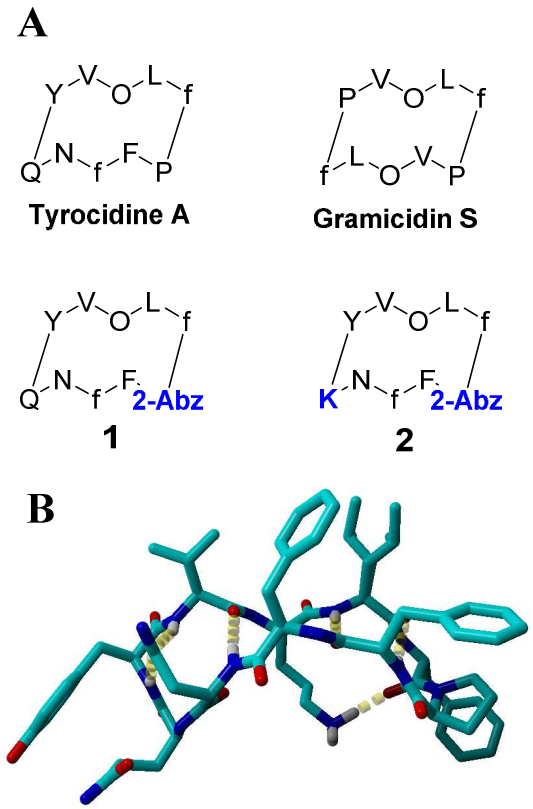

Figure 1: (A) Amino acid sequences of Tyrc A, gramicidin S and, compounds **1**and **2**. D-Amino acids are represented by lower case letters. 2-Abz represents 2-aminobenzoic acid and O represents ornithine. Bold letters are used to denote amino acids altered in the analogues. (B) Crystal structure of Tyrc A, showing hydrogen bonds; taken from PDB ID: 4M6E.[5]

Results and Discussion

The turn nucleated by D-Phe[1]-Pro[2] in Tyrc A was replaced with the D-Phe-2-Abz turn motif. The additional backbone atom in 2-Abz and rigidity imparted by this residue was expected to result in an altered molecular architecture, allowing us to gain new insights as to how the conformation influences the biological properties of the molecule. Antibacterial activity was investigated against *E. coli, P. aeruginosa* and *S. aureus* by minimal inhibitory concentration (MIC) analyses and toxicity measured by haemolysis of mouse red blood cells (RBCs). The novel Tyrc A

analogue, compound **1** (Figure 1), was approximately 30-fold less haemolytic than Tyrc A (Figure 2). However, its antibacterial activity against *S. aureus* was moderately reduced (four-fold, Table 1).

Table 1: Antibacterial activity of Tyrc A and analogues **1**-**2**

Compound	MIC (μM)[a]		
	E.coli	*P. aeruginosa*	*S. aureus*
Tyrc A	25	100	1.56
1	50	100	6.25
2	12.5	25	1.56

[a] MIC determined from three independent experiments each with three internal replicates.

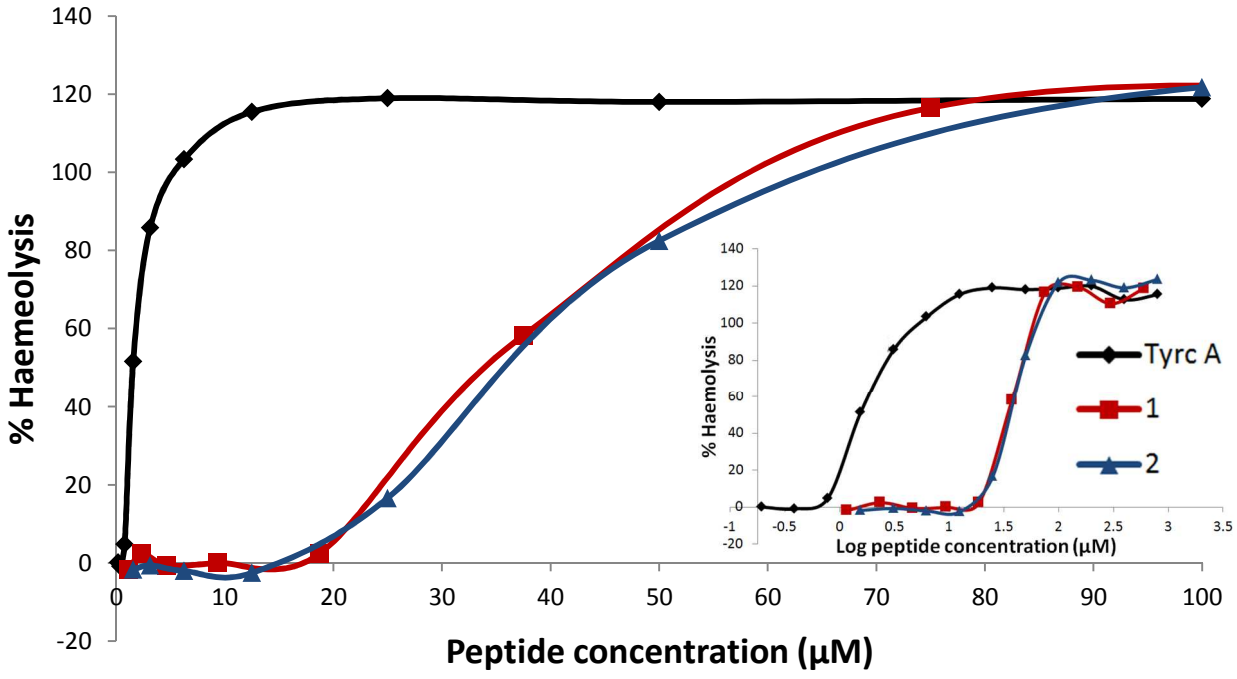

Figure 2: Percentage of haemolysis of mouse blood cells at various concentrations of Tyrc A and compounds **1** and **2**. 100% haemolysis referenced as treatment with 0.5 % triton X-100. Inset: percentage haemolysis plotted against log peptide concentration (μM).

Compound **1** was poorly soluble in water and therefore a 1:1 mixture of CD_3CN and H_2O was chosen for nuclear magnetic resonance (NMR) studies. Well dispersed resonances were observed in this solvent mixture (Figure S3; Table S2). Additionally, this solvent system may better mimic the interaction of the peptide with biological membranes than aqueous conditions. Strong $C^{\alpha}_{i}H$ – $N_{i+1}H$ rotating frame Overhauser effects (ROEs) and large $^{3}J_{NH\text{-}C\alpha H}$ coupling constants, ranging from 7.3 - 8.8 Hz were observed for the β-strand residues (Phe^{3}-Asn^{5} and Val^{8}-Leu^{10}), supporting an extended backbone conformation typical of β-sheets. A diagram highlighting key inter-strand ROEs observed for the cyclic β-hairpin **1** is shown in Figure S4. Structures were calculated with experimentally derived ROE restrains using the standard NMR structure calculation protocol of the YASARA molecular modelling package. The ensemble of calculated structures showed a conformational shift, for compound **1**, to a more planar architecture than Tyrc A (Figure 3). The increased planarity sees the hydrophilic Tyr^{7} residue drifting towards the hydrophobic upper face, while the hydrophilic Asn^{5} residue also shifts and now resides directly on the upper face (Figure 3). Furthermore, the Phe^{3} side chain shifts away from the hydrophobic face towards the lower face which is predominantly hydrophilic for Tyrc A. All nine ensemble members demonstrated a similar geometry with a root mean square deviation (RMSD) average of only 0.98 Å for the total structure (Figure 4). Both the increased planarity of the backbone and side chain shifts, especially that of Phe^{3}, result in a reduction in the amphipathic organisation of the molecule and in-turn, appear responsible for the reduced haemolysis of compound **1**. In

support of the reduced hydrophobic upper face presented by compound **1**, the reversed-phase high performance liquid chromatography (RP-HPLC) retention time of this compound was reduced approx. 5 minutes compared to Tyrc A even on a gradient with reduced solvent B (Table S1).

Given the Gln^6 side chain is oriented towards the cationic face in both **1** and Tyrc A (Figures 3 and 4) and is not involved in stabilising the intramolecular structure or dimerization of Tyrc A[5], it appeared a good candidate for substitution in order to improve the antibacterial activity of **1**. In-fact, a simple point substitution of Gln^6 for lysine in Tyrc A was reported by Marquez *et al*[8]. While they found this substitution to enhance the already potent activity against Gram positive bacteria, little or no advantage was achieved for the Gram negative *E.coli* with MICs >100 μM. Effect of this substitution on haemolysis was not reported.

In an attempt to improve the antibacterial activity of **1**, we synthesised compound **2** where Gln^6 in **1** was substituted with lysine (Figure 1). To our delight we found that the reduced haemolysis of **1** (approx. 30 fold) was maintained by compound **2** (Figure 2) while the spectrum of activity was broadened and potency enhanced (Table 1). Activity of **2** against *S. aureus* was equivalent to that of Tyrc A (MIC of 1.56 μM) and also increased by two and four fold against *E. coli* and *P. aeruginosa* and respectively (Table 1).

The NMR structure of compound **2** (NMR parameters given in Table S3) demonstrated a structural shift from Tyrc A to a more planar architecture nearly identical to that of compound **1** (Figure 3). The structural similarity is supported by the observation of many key intra- and inter-stand ROEs common to both compounds **1** and **2** (Figures S4-5). The ensemble of eight structures for compound **2** was also well defined (Figure 4), demonstrating an RMSD average of only 1.12 Å for the total structure. The conserved structure of compound **2**, relative to its predecessor, compound **1**, supports our observation that the D-Phe-2-Abz turn is responsible for the reduction in haemolysis of compounds **1** and **2**, by means of increased ring planarity and side chain shifts that ultimately disrupts amphipathicity and hydrophobicity of the upper face (Figures 3 and 4). In further support of this argument, Gln^6 substitution for ornithine (Orn) or Lys in Tyrc A, documented by Qin *et al*[17], provided much lesser reductions in haemolysis (3 or 12-fold respectively) than observed for compounds **1** and **2** (approx. 30-fold). Similar observations on amphipathic disruption have been previously reported for designed AMPs whereby, substitutions leading to a less well-defined amphipathic character resulted in reduced haemolysis.[18] The enhanced activity of **2** (compared to **1**) is then attributable to the increased cationic charge of the lower face where both Lys^6 and Orn^9 now reside (Figures 3, and 4). This is in accordance with previous Tyrc A analogues, in which point substitution of cationic residues on the hydrophobic upper face saw reduced haemolysis, while their introduction to the lower face predominantly increased antibacterial activity.[8, 19-20] The crystal structure of Tyrc A appears to accurately represent the bioactive conformation in solution, as it supports the results of previous structure-activity-relationship studies based on point substitutions.[5, 8] While the changes in amphipathicity for the calculated structures of compounds **1** and **2** account for both the observed changes in

bioactivity and reduced HPLC retention time of **1**, it should be noted that there is of course potential for discrepancy when comparing NMR and crystal structures.

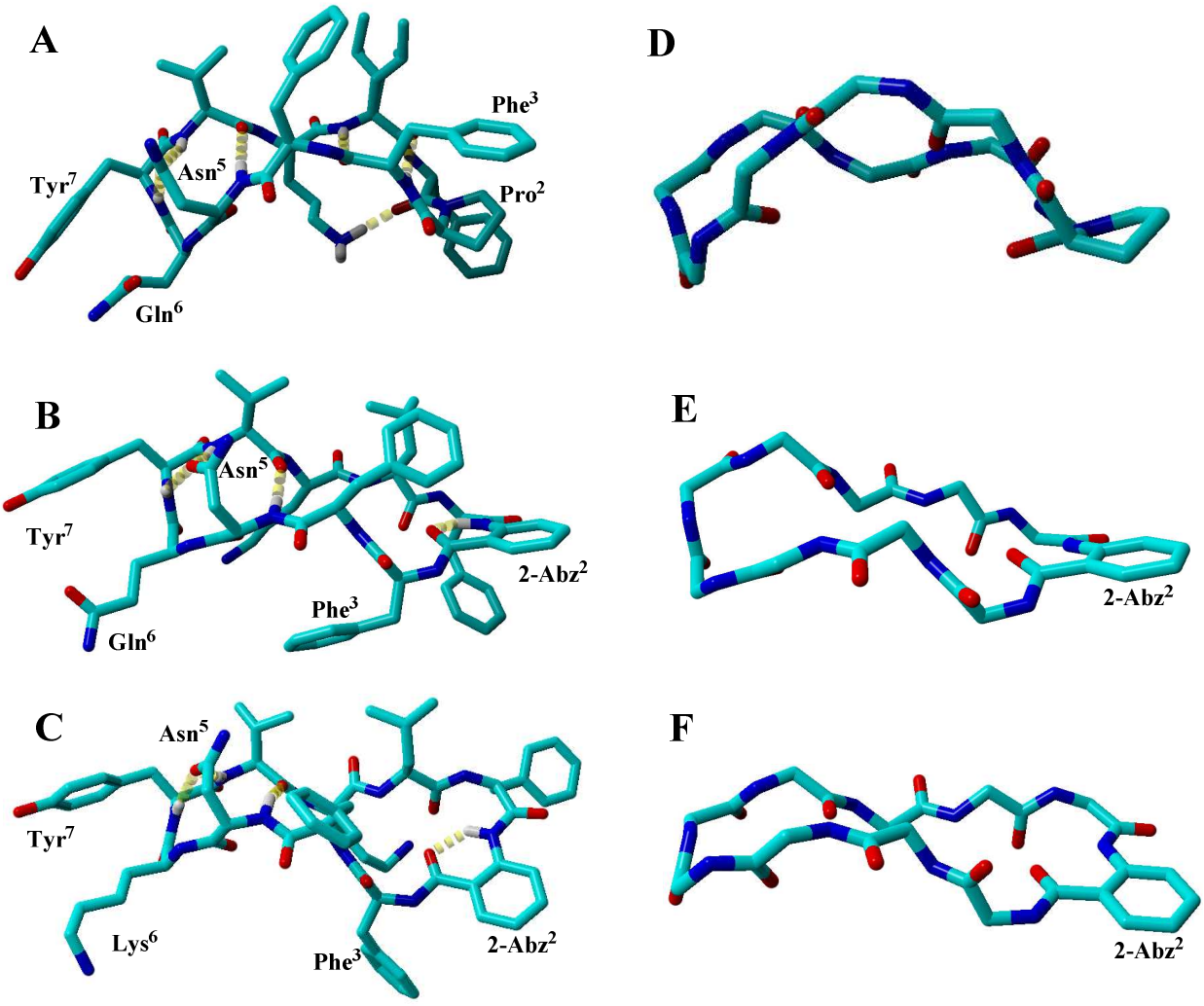

Figure 3: Left; Perspective views showing hydrogen bonds, for the crystal structure of Tyrc A (A) and single representative NMR structure calculated for **1** (B) and **2** (C). Right; the backbone of each molecule is shown with side chains removed to highlight the curvature of Tyrc A (D) and the greater planarity of both **1** (E) and **2** (F). The crystal structure of Tyrc A was taken from PDB ID: 4M6E.[5]

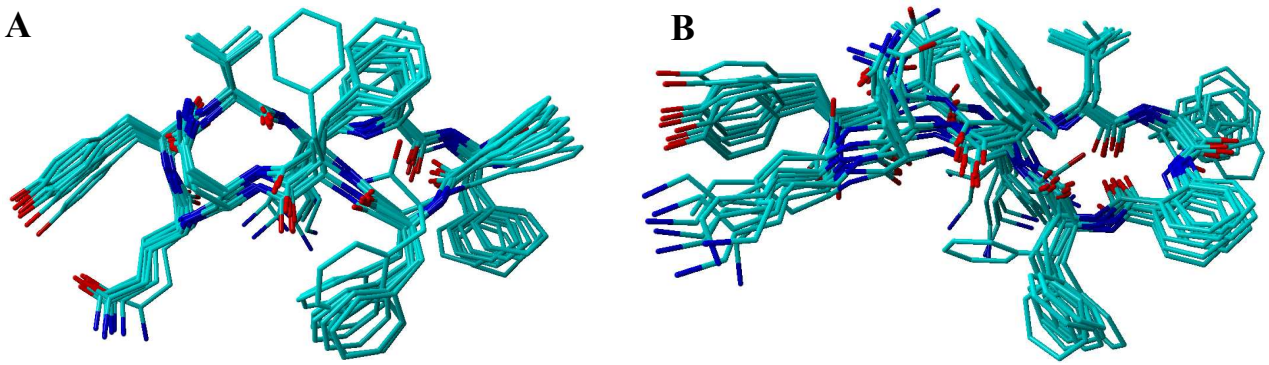

Figure 4: Ensemble of lowest energy NMR structures calculated for compound **1** (A) and compound **2** (B) showing nine and eight structures respectively. The predicted $^{3}J_{NH\text{-}C\alpha H}$ values of the calculated structures were generally in good agreement with the experimentally determined values (Tables S2 and S3).

While previous efforts by Kohli *et al*[19] to enhance the therapeutic index of Tyrc A by making point substitutions provided two compounds with significantly reduced haemolysis, the activity of both was compromised against Gram positive bacterial strains (approx. four and nine-fold against MRSA) and remained poor or moderate respectively against two Gram negative pathogens, *E. coli* (120 µM and 290 µM) and *P. aeruginosa* (30 µM and 37 µM). On the other hand, compound **2** reported here, possessing an altered turn framework and molecular architecture, reduces haemolysis approx. 30-fold while also enhancing activity against Gram negative species and retaining potency against Gram positive *S. aureus*. Thus, the improved bioactivity properties of compound **2** highlights the potential therapeutic applications of peptides employing the D-Phe-2-Abz turn motif.

As stated above, the β-turn nucleated by the D-Phe-2-Abz motif is almost identical for compounds **1** and **2** (Figure 3). This β-turn structure demonstrated similar $C^{\alpha}_{i} - C^{\alpha}_{i+3}$ distances to Tyrc A and is shown for compound **2** alongside the turn structure of Tyrc A (Figure 5). Crucially, the full ensemble of compound **2** (Figure 4) demonstrated appropriate $C^{\alpha}_{i} - C^{\alpha}_{i+3}$ distances of 5.39 – 5.78 Å satisfying the 7 Å limit used for defining β-turns.[21-23] The D-Phe-2-Abz motif demonstrates an intra-residue hydrogen bond (H-bond) of 2-Abz which stabilises the planar conformation and appears to constitute a minimal β-turn motif (Figures 3 and 5). Stabilisation of the 2-Abz geometry by this intra-residue H-bond has previously been observed in both the crystal and solution states by the Sanjayan group.[10-11] Despite both compounds **1** and **2** maintaining a β-turn with a similar $C^{\alpha}_{i} - C^{\alpha}_{i+3}$ distance to native Tyrc A (Figure **5**), a shift in geometry about Leu[10], Phe[3] and the N-terminus of D-Phe[4] sees only one of the three inter-strand backbone H-bonds of Tyrc A maintained, between Asn[5] NH and the carbonyl of Val[8] (Figure 3). However, despite the reduction in inter-strand H-bonds, the well-defined (low RMSD) ensembles of both analogues suggest a robust and rigid framework is maintained in the presence of the D-Phe-2-Abz turn motif. At the other end of the molecule, the bifurcated H-bond of the Asn[5] side chain carbonyl to the NH of both Tyr[7] and Val[8] is maintained similarly to Tyrc A, despite the increased backbone planarity of these analogues (Figure 3). This side chain-backbone interaction appears to stabilise both the β-turn and side chain conformation at this end of the molecule (Figure 4). Additionally, like Tyrc A, ensemble members of both analogues demonstrated possible backbone H-bond contacts for the Orn[9] side chain on the lower face of the molecules (not shown). The H-bonds observed in the modelled structures of compounds **1** and **2** (Figure 3) are further supported by low amide temperature coefficients ($d\delta/dT$) of 2-Abz[2], Asn[5],

Tyr[7] and Val[8], ranging -2.4 to -4.2 ppb/K, compared to that of D-Phe[1] (-7.6 and -7.3 ppb/K) which was not predicted to form any H-bond contacts and appears solvent exposed.[24-25] The temperature coefficient of Leu[10] was also surprisingly low (approx. -1 ppb/K). This could be explained by a weaker H-bond occurring between the NH of Leu[10] and the carbonyl of 2-Abz-[2] (Figure 5). For compound **2** donor – acceptor distances ranging 3.4 – 3.8 Å were observed for this interaction in all eight ensemble members, while for compound **1,** this interaction appears less likely with donor – acceptor distances slightly > 4 Å. The occurrence of this i – i+2 H-bond is in accordance with our previous observations from the crystal structure of the model β-turn tetrapeptide D-leu-D-Phe-2-Abz-D-Ala.[14] The temperature coefficients of the Gln[6] / Lys[6] amides were also relatively low, - 3.9 and -4.3 ppb/K for compounds **1** and **2** respectively. Based on the modelled structures, it appears unlikely this is due to any H-bonding interaction and instead may be due to solvent shielding by the Asn[5] side chain. Similar effects of side chains have been previously observed for cyclic peptides and may also contribute to the low temperature dependence of Leu[10].[24, 26]

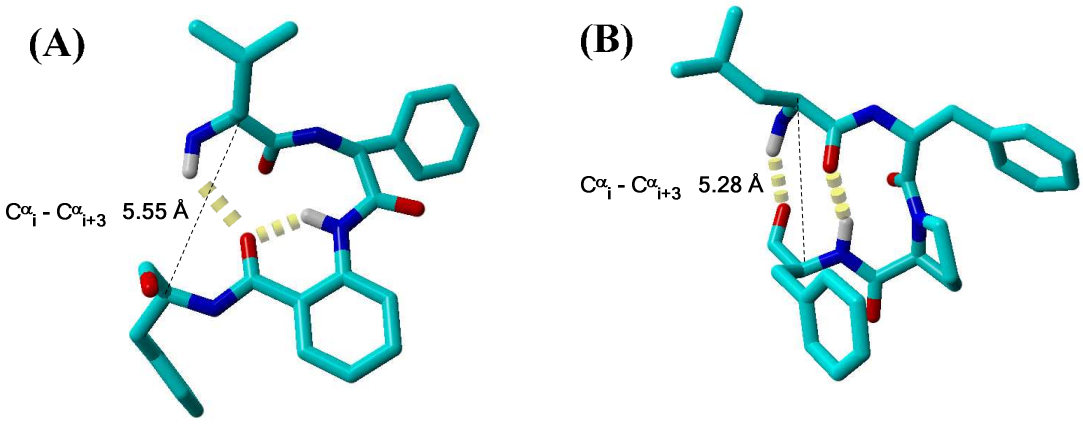

Figure 5: (A) Representative molecule from the ensemble of **2** showing β-turn structure induced by the D-Phe-2-Abz motif. The intra-residue H-bond of 2-Abz[2] and a likely i – i+2 H-bond

between the D-Leu[10] amide and carbonyl of 2-Abz[2] are also shown. (B) Crystal structure of Tyrc A showing the β-turn induced by the D-Phe-Pro motif, with the alternate Leu conformation removed. The $C^{\alpha}_{i} - C^{\alpha}_{i+3}$ distance of each (A and B) is highlighted. The crystal structure of Tyrc A was taken from PDB ID: 4M6E.[5]

The antibacterial mode of action of compound **2** and synthetic Tyrc A was investigated by TEM against both *S. aureus* and *P. aeruginosa* (Figures 6 and 7). *S. aureus* control cells showed relatively uniform and intact cell membranes and cell walls. The cell wall was noted to be slightly diffuse in areas, particularly for dividing cells (Figure 6, right).[27] The intracellular area consistently demonstrated high density and in some sections, particularly dividing cells, genetic material (nucleoid) was clearly seen.[27-29] However, *S. aureus* cells with ruptured cell membranes and cell walls were consistently observed after one hour treatment with both Tyrc A and compound **2**.[5] Peptide treated cells consistently showed reduced intracellular density, suggesting cellular leakage, even when the section did not reveal obvious membrane damage (Figure 6, right). The observations from the TEM images are consistent with those of other studies employing either transmission or scanning electron microscopy (SEM).[15-16, 30-32]

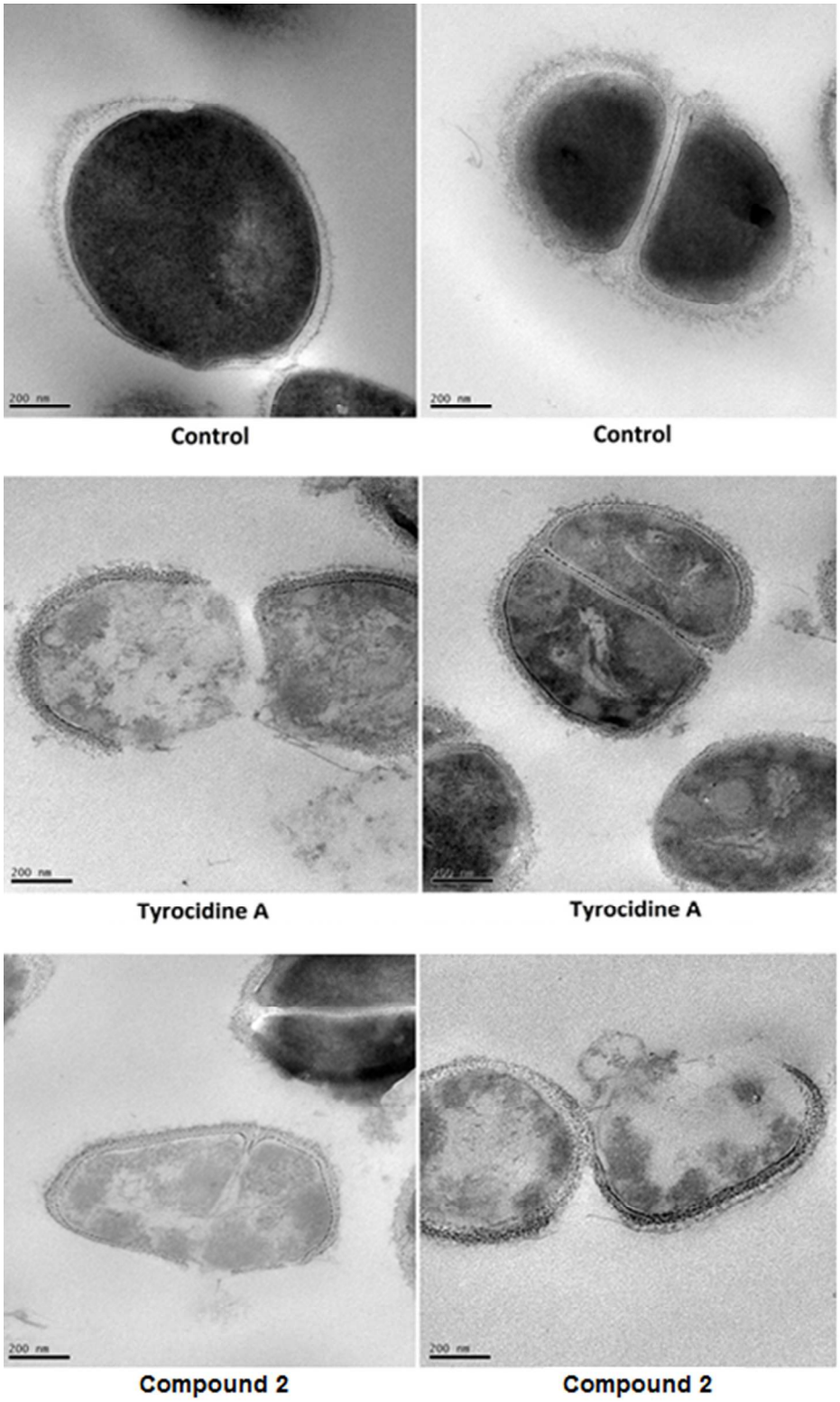

Figure 6: TEM micrographs of *S. aureus* untreated (control) or treated with Tyrc A and compound **2**.

P. aeruginosa control cells consistently demonstrated smooth in-tact cell membranes. Staining of the intracellular space was less consistent than for *S. aureus*, particularly towards the centre of the cells where the stains may not have penetrated (Figure 7). Despite treatment with Tyrc A at 4 X MIC, *P. aeruginosa* cells failed to demonstrate any obvious membrane disruption. The cells did however demonstrate enhanced uptake of the stain, suggesting increased membrane permeability. This appears consistent with the poor potency (high MIC) of Tyrc A against this pathogen. On the other hand, cells treated with compound **2** (4 X MIC) consistently demonstrated blebbing and total membrane lysis. Again, this is consistent with both SEM and TEM studies of AMPs previously reported.[15-16, 30-32]

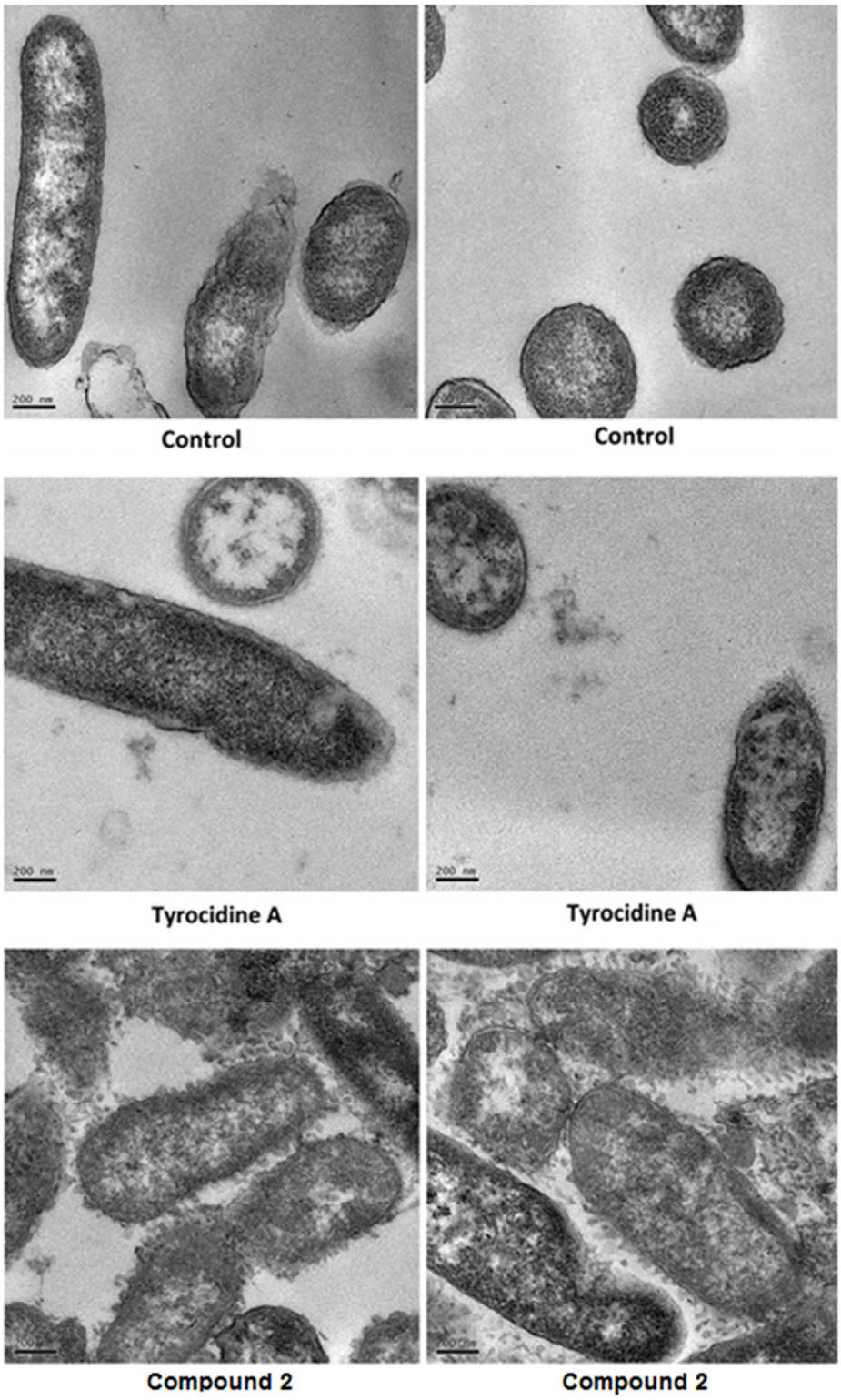

Figure 7: TEM micrographs of *P. aeruginosa* untreated (control) or treated with Tyrc A and compound **2**.

Tyrc A is strongly suggested to interact with bacterial membranes as a dimer which accentuates the amphipathic structure.[5, 33] As reported previously by Munyuki *et al*[33], intermolecular dimers were observed for TyrcA by electrospray ionization mass spectrometry (ESI-MS), with similar observations occurring for both compounds **1** and **2** (Figure S2). This data suggested compounds **1** and **2** may interact with bacterial membranes by a mechanism similar to Tyrc A. The presence of a doubly charged dimeric species in the ESI-MS spectra raised the question as to whether cyclodimerisation had occurred during synthesis. However, mass spectrometry analysis by matrix-assisted laser desorption/ionization time of flight (MALDI-TOF) did not detect the dimeric species (data not shown) and presence of the cyclic monomer was further confirmed by NMR spectroscopy for **1** and **2**.

Antifungal susceptibility testing of compound **2** and Tyrc A was performed against *C. albicans* (Table 2). Tyrc A is known to possess membrane lytic activity against fungi, however evidence has strongly suggested additional antifungal targets.[2-3] Tyrc A is also known to act synergistically with amphotericin B.[3] Tyrc A demonstrated an MIC of 3.125 μM, while compound **2** showed an MIC of 12.5 μM. However, in the presence of sub-MIC concentrations (0.39 μM and 0.78 μM) of amphotericin B, known to induce pores in fungal membranes, compound **2** displayed a synergistic effect with potency equivalent to that of Tyrc A, with both showing MICs in the nanomolar range against *C. albicans* (Table 2). Presumably this occurs by either a cooperative membrane lytic mechanism or by enhanced membrane permeability, induced by amphotericin B, promoting access to additional intracellular targets. While highly effective,

clinical use of amphotericin B is limited by nephrotoxicity, primarily due to a lack of selectivity between fungal and mammalian membranes.[34-35] Therefore the development of synergistic antifungal strategies allowing lower and less toxic doses of amphotericin B is of great value.

Table 2: Antifungal activity of Tyrc A and compound **2**, showing synergism with Amphotericin B.

Compound	MIC (μM)[a]		
	C. albicans	*C. albicans* + 0.39 μM AMB[b]	*C. albicans* + 0.78 μM AMB[b]
Tyrc A	3.125	0.78	0.39
2	12.5	0.78	0.39
Amphotericin B	1.56	N/A	N/A

[a] MIC determined from three independent experiments each with three internal replicates.

[b] Media supplemented with sub-MIC concentration of amphotericin B.

Conclusions

NMR structures of compounds **1** and **2** demonstrated that the D-Phe-2-Abz motif can be used as a minimal β-turn motif replacing the D-Phe-Pro β-turn of Tyrc A, maintaining similar $C^{\alpha}_{i} - C^{\alpha}_{i+3}$ distances. Compound **2** is a novel Tyrc A analogue that displays a broader spectrum of antibacterial activity with increased potency against Gram negative pathogens, approximately 30-fold reduced haemolysis and antifungal activity in the nanomolar range when used in synergy with amphotericin B. Although the biological properties of compound **2** are significantly more

favourable than those of the parent Tyrc A, further fine tuning of the structure would be required before real therapeutic value can be realised. Nevertheless, both compounds **1** and **2** provide novel insights into the relationship between the molecular conformation and bioactivity of Tyrc A, whereby substitution of proline for 2-Abz lead to significantly altered physical and biological properties due to a shift in the molecular architecture. The D-Phe-2-Abz turn motif presents a framework that is likely to accommodate different amino acids with varied side chain characteristics and stereo-configurations in the i and i+3 positions for the generation of β-hairpin libraries, much like the common D-Pro-Gly turn. Furthermore, compared with existing turn motifs such as D-Pro-Gly, potential for ring substitutions on 2-Abz greatly expands the scope to display further functionalities or create conjugates without side chain flexibility. The D-Phe ring may also anchor additional functional groups via substitution with D-Tyr or more complex structures.

Experimental

Chemicals and Reagents

All Fmoc-amino acids, 1-(bis-(dimethylamino)methylene)-1H-1,2,3-triazolo[4,5-b]-pyridinium 3-oxide hexafluorophosphate (HATU) and (3-Hydroxy-3H-1,2,3-triazolo[4,5-b]pyridinato-O)tri-1-pyrrolidinyl-phosphorushexafluorophosphate PyAOP were purchased from AK scientific, USA. 2-chlorotritylchloride resin was purchased from Peptides International, USA. *N*,*N*-diisopropylethylamine (DIPEA), piperidine, and other common solvents were purchased from Sigma Aldrich, NZ. Mueller Hinton broth (MHB, non-cation adjusted) of BD-Difico brand was purchased from Fort Richard Laboratories, New Zealand.

Peptide Synthesis and Purification

Linear peptides were synthesised on the 2-chlorotrityl chloride resin following standard Fmoc solid phase peptide synthesis protocols at 0.1 mmol scale using N,N-dimethylformamide (DMF) as the solvent. Amino acid side chains were protected as follows, asparagine: trityl (Trt), glutamine: trityl (Trt), lysine: *tert*-butyloxycarobonyl (Boc), ornithine: *tert*-butyloxycarobonyl (Boc), tyrosine: *tert*-butyl (*t*Bu). Fmoc deprotections were performed using 20 % piperidine in DMF twice for 10 minutes each using a large excess. Each coupling reaction was performed using HATU (144.4 mg, 0.38 mmol, 3.8 eq.) and the respective amino acid in 4-fold excess with DIPEA (175 µl, 1 mmol, 10 eq.) as the base. Couplings to 2-Abz were performed for 3 h. Protected linear peptides were cleaved from the resin using 1 % trifluoroacetic acid (TFA) in dichloromethane (DCM, 10 mL). TFA cleavage was performed repeatedly for five times of 1 min duration each with washings collected into a flask already containing triethylamine (1.5 molar excess to the total TFA). Crude linear peptides were purified to > 95 % purity by RP-HPLC. Percentage yields of the linear peptides after purification were 11.5 (**1**), 15.2 (**2**) and 45 (TyrcA) respectively. RP-HPLC was undertaken using a GE Pharmacia ÄKTA purifier 10 system with a Phenomenex Luna 5 µm C18 100 Å (250 mm × 21.2 mm) column, using H_2O with 0.1% TFA as solvent A and 99 % MeCN 1% H_2O with 0.1 % TFA at a flow rate of 10 mL/min with UV detection at 214, 254 and 280 nm (Table S1). Purified peptides were obtained as white fluffy solids after lyophilisation. For cyclisation, the protected linear peptides were dissolved in DMF at 1.25 mM with 1 % v/v of DIPEA. After stirring for 5 min, PyAOP (3 eq.) was added and the reaction allowed to proceed for 4 h before removal of the solvent under vacuum. The crude cyclic peptides were deprotected using TFA:H_2O:TIS cocktail (95:2.5:2.5) for 3 h. The crude cyclic product was purified to > 95 % purity by RP-HPLC using a linear gradient of H_2O and

MeCN. Purified cyclic peptides were obtained as white solids after lyophilisation. Purity of peptides was confirmed by analytical RP-HPLC (Figure S1) using a Phenomenex Luna 5 µm C18 100 Å (250 mm × 4.6 mm) column and 0.5 mL/min flow rate. The identity of the purified peptides was confirmed using electrospray ionization mass spectrometry (ESI-MS) recorded on a Bruker micrOTOFQ mass spectrometer (Figure S2). ESI-MS demonstrated a small peak corresponding to the intermolecular dimer for compounds **1**, **2** and Tyrc A, in accordance with literature.[33] However cyclodimers were not detected after dilution and were absent in MALDI-MS.

NMR Spectroscopy

Compounds **1** and **2** were dissolved in a 1:1 mixture of CD_3CN (Cambridge Isotopes, 99.8%) and MQ-H_2O at 0.7 mM and 0.8 mM respectively. NMR spectra were recorded on a 5 mm, TCI cryoprobe-equipped with Bruker Avance 700 spectrometer operating at 700.13 MHz. Peak assignments were made using 2D double-quantum filtered COSY and TOCSY spectra (mixing time 80 ms). Distance restraints were obtained from ROESY spectra (mixing time150 ms and relaxation delay of 3 s). All 2D NMR spectra were recorded at 298 K. 1D ^{1}H NMR spectra were obtained at 5 K intervals between 288 K and 318 K in order to establish the temperature dependence of the NH chemical shifts. Spectra were referenced relative to an external standard of the solvent spiked with TMS at 0 ppm and measured at each temperature.

Spectra were processed with Bruker Topspin 2.1.8 using standard parameters. Peak assignments and generation of ROE distance restraints was performed using CCPN Analysis v.2.4.2.[36] Peak

volumes were calculated using standard settings and ROE distances were calibrated by setting the average volume of the D-Phe H_β protons to 1.8 Å.

Solution Structure Calculation

Structures of compounds **1** and **2** were calculated using the standard NMR structure calculation protocol of the program YASARA[37] as described.[38] In short, the ROE restraints were exported from CCPN Analysis in XPLOR format and included in structure calculations in all steps. Calculations additionally included dihedral angle restraints deduced from coupling constants ($^3J_{NH\text{-}C\alpha H}$). The dihedral angles for phi were calculated using the Karplus equation.[39] As can be seen in the angular dependence of $^3J_{NH\text{-}C\alpha H}$ values published by Pardi *et al*[40], there is a clear maximum in the distribution at phi = -120° corresponding to J = 9 Hz. This means for J ≥ 9 Hz phi is well defined. However, for the smaller $^3J_{NH\text{-}C\alpha H}$ values, phi can be a within a range, such as for example -120±40° for J = 7 Hz. Therefore, we defined our phi angles loosely as phi = -120 ± (25-35)° depending on the observed coupling constant and as phi = -60 ± 20° for residue 6 (observed $^3J_{NH\text{-}C\alpha H}$ = 4.51 or 4.29) in both compounds. As an extra control, we first calculated structures based only on distance restraints. The introduction of dihedral angles restraints did not result in ROE violations nor did it change the secondary structure significantly. A hydrogen bond between two strands was set according to the ROE pattern for both compounds **1** and **2** (Supplementary Figures S4 and S5). First, ten roughly folded structures were calculated by randomly changing torsion angles starting from the initial structure built with D-amino acids and non-standard amino acids. The structures were refined in vacuum by running restrained molecular dynamic simulations in the NOVA force field.[37] The protocol involved 40 cycles of heating and cooling (simulated annealing). Afterwards, to improve the quality of the structures,

they went through water refinement using the same restraints. The structures with the lowest energy and retaining D-configuration (where appropriate) were chosen from 10 structures to represent the ensemble for each compound. We observed only one ROE from the possible dimerization of compound **1**. This is the ROE between Tyr 7 and Phe 1 and corresponds to the dimeric interaction observed in Tyrc A crystal structure.[5] This ROE was excluded from calculation, as it was conflicting with other ROEs in the derived monomer structures. We did not observe other dimeric ROEs, consistent with the expectation of the dimer being less stable in solution than in the crystal structure. Due to the lack of dimeric ROEs, only monomeric structures could be calculated. Additionally, the expected dimeric ROEs from Tyrc A dimerization, are incompatible with a monomeric structure. Exclusion of the single observed dimeric ROE from the calculation resulted in structures consistent with the majority of ROEs. Additional data pertaining to structure calculation can be found in Table S4.

Bacterial Minimal Inhibitory Concentration Assay (MIC)

S. aureus, E. coli and *P. aeruginosa* were incubated at 37 ^{o}C overnight in MHB (non-cation adjusted). The overnight bacterial cultures were adjusted to an OD of 0.1 and further diluted 1:100 in accordance with a documented literature protocol.[41] Assays were performed on 96-well microtitre plates preparing dilutions in the plates prior to bacterial inoculation. Plates containing 50 µl of the compounds at twice the final test concentrations (or media alone for the non-treated growth control) were inoculated with 50 µl of the diluted bacterial suspension. The sterility control contained just 100 µl of the media. After incubation at 37 ^{o}C for 18 h, optical density at 600 nm was measured using a plate reader. MIC was defined as the lowest concentration in

which no bacterial growth was observed as determined from three concordant experiments, each with three internal replicates.

Fungal Minimal Inhibitory Concentration Assay (MIC)

Fungal susceptibility testing was performed following a literature procedure with minor changes.[42] A single colony of *C. albicans* was transferred to a solution of Roswell Park Memorial Institute (RPMI) media (0.5 ml) and adjusted to an OD of 0.1 and then diluted 1:100. The assay was conducted as per bacterial MIC assays with the incubation period increased to 48 hours. The MIC determination was performed by visual inspection as the fungus does not grow as a homogeneous solution for plate reading; instead colonies on the bottom of the wells are observed. MIC was defined as the lowest concentration in which no fungal growth was observed as determined from three concordant experiments, each with three internal replicates. Synergistic assays were performed, using media supplemented with amphotericin B (0.78 or 1.56 μM) with the various compound dilutions in the plate resulting in a final amphotericin concentration of 0.39 and 0.78 μM in each well of the plates.

Haemolysis Assay

Haemolysis of the peptides was tested by determining the haemoglobin release from erythrocyte suspensions of fresh mouse blood (2 %, v/v). Blood was collected under the University of Auckland's Animal Ethics Committee's approval titled "Animal tissue and blood harvesting, Production of antisera and/or antibodies" for scientific investigations. The strain of mouse used

was ICR - CD-1. The blood cells were centrifuged for 5 min and the plasma was removed. The blood cells were washed in Tris buffer (10 mM Tris, 150 mM NaCl, pH 7.2) and the pellet re-suspended in the Tris buffer (2 % v/v). A two-fold dilution series of the peptides in Tris buffer was made in the 96-well microtitre plate. To these peptide solutions (50 µL) were added re-suspended blood cells (50 µL) and the plates incubated without shaking at 37 ^{o}C for 1 h. Neat buffer and 0.5 % Triton X-100 (50 µL) served as the controls. The experiment was performed in triplicates. After 1 hour, the plates were centrifuged at 3500 x g for 10 min. The supernatant (80 µL) from each well was transferred into fresh 96 well plates and absorbance at 540 nm measured. Percentage haemolysis at a given concentration of the peptide was calculated from the following equation, where A_{exp} is the experimental A_{540} measurement, A_{Tris} is the negative control where only Tris buffer was added to RBC, and $A_{100\%}$, is the positive control where 0.5 % Triton X-100 (50 µL) was used to cause lysis of 100 % RBC present.

$$\% \text{ haemolysis} = (Aexp - ATris)/(A100\% - ATris) \times 100$$

Transmission Electron Microscopy (TEM)

S. aureus and *P. aeruginosa* were grown as overnight cultures in MHB (non-cation adjusted). Bacterial suspensions were diluted to an OD of 0.4 in MHB. A 1 mL aliquot of each bacterial suspension was used for each sample preparation. Control samples were incubated for one hour at 37 ^{o}C, while the peptide treated samples were incubated for one hour with each compound at 4 x MIC. After incubation the cells were centrifuged and washed thrice at 5000xg for 3 min with Tris buffer (10 mM Tris, 150 mM NaCl, pH 7.4). The pellets were then re-suspended in a 4% gluteraldehyde solution in the buffer and incubated at room temperature for 2 hours. The fixed

cells were then centrifuged and washed thrice at 5000xg for 3min with Tris buffer. The washed cells were post-fixed with 1% osmium tetroxide in PBS for 1 hour. The post-fixed cells were then dehydrated through a graded ethanol series (50, 90 and 100%) before placing in absolute acetone twice for 10 min each. The supernatant was removed and replaced with a 1:1 mixture of absolute acetone and epoxy resin for 1 h before transfer to pure epoxy resin for overnight. The pellets were then transferred into appropriate tubes and incubated at 60 ^{o}C for 48 h before ultrathin sections were obtained using an ultramicrotome. The sections were post-stained with uranyl acetate and lead citrate. Samples were viewed by transmission electron microscopy (FEI Technai 12).

Acknowledgments

We thank Stefan Harjes for help with YASARA. AC thanks the University of Auckland and Freemasons New Zealand for Doctoral Scholarships.

Abbreviations

2-Abz, 2-aminobenzoic acid (anthranilic acid); AMP(s), antimicrobial peptide(s); DBU, 1,8-Diazabicyclo[5.4.0]undec-7-ene; DCM, dichloromethane; DMF, *N,N*-dimethylformamide; DIPEA, *N,N*-diisopropylethylamine; ESI-MS, electrospray ionization mass spectrometry; Fmoc, 9-fluorenylmethyloxycarbonyl; H-bond, hydrogen bond; HATU, 1-(bis-(dimethylamino)methylene)-1H-1,2,3-triazolo[4,5-b]-pyridinium 3-oxide hexafluorophosphate; MALDI-TOF, matrix-assisted laser desorption/ionization time of flight; MeCN, acetonitrile;

MHB, Mueller-hinton broth; MIC, minimal inhibitory concentration; MRSA, methicillin resistant *Staphylococcus aureus*; 2-NBS-Cl, 2-Nitrobenzenesulfonyl chloride; NMP, N-methylpyrrolidinone; Orn, ornithine; RBC, red blood cells; ROE, rotating frame Overhauser effect; RMSD, root mean square deviation; RP-HPLC, reversed phase high pressure liquid chromatography; RPMI, Roswell Park Memorial Institute SEM, scanning electron microscopy; TEM, transmission electron microscopy; TFA, trifluoroacetic acid, TIS, triisopropyl silane; Tyrc A, tyrocidine A.

ASSOCIATED CONTENT

Supporting Information

The Supporting Information is available free of charge on the ACS Publications website.

Physical characteristics of peptides, analytical HPLC traces, ESI-MS spectra, NMR parameters and spectra, PDB files for compounds **1** (PDBID: 6B34) and **2** (6B35)

SMILES Molecular formula strings (csv file)

Coordinates and experimental data for the compounds **1** and **2** have been deposited with the Protein Data Bank (www.rcsb.org/pdb) under accession codes 6B34 and 6B35 respectively. Authors will release the atomic coordinates and experimental data upon article publication.

References

1. Bu, X.; Wu, X.; Xie, G.; Guo, Z. Synthesis of Tyrocidine A and Its Analogues by Spontaneous Cyclization in Aqueous Solution. *Org. Lett.* **2002,** *4* (17), 2893-2895.

2. Rautenbach, M.; Troskie, A. M.; Vosloo, J. A.; Dathe, M. E. Antifungal membranolytic activity of the tyrocidines against filamentous plant fungi. *Biochimie* **2016,** *130*, 122-131.

3. Troskie, A. M.; Rautenbach, M.; Delattin, N.; Vosloo, J. A.; Dathe, M.; Cammue, B. P. A.; Thevissen, K. Synergistic Activity of the Tyrocidines, Antimicrobial Cyclodecapeptides from Bacillus aneurinolyticus, with Amphotericin B and Caspofungin against Candida albicans Biofilms. *Antimicrob. Agents Chemother.* **2014,** *58* (7), 3697-3707.

4. Robinson, J. A. β-Hairpin Peptidomimetics: Design, Structures and Biological Activities. *Acc. Chem. Res.* **2008,** *41* (10), 1278-1288.

5. Loll, P. J.; Upton, E. C.; Nahoum, V.; Economou, N. J.; Cocklin, S. The high resolution structure of tyrocidine A reveals an amphipathic dimer. *Biochim. Biophys. Acta* **2014,** *1838* (5), 1199-1207.

6. Joo, S. H. Cyclic Peptides as Therapeutic Agents and Biochemical Tools. *Biomol. Ther.* **2012,** *20* (1), 19-26.

7. Rammelkamp, C. H.; Weinstein, L. Toxic effects of tyrothricin, gramicidin and tyrocidine. *J. Infect. Dis.* **1942,** *71* (2), 166-173.

8. Marques, M. A.; Citron, D. M.; Wang, C. C. Development of Tyrocidine A Analogues with Improved Antibacterial Activity. *Bioorg. Med. Chem.* **2007,** *15* (21), 6667-6677.

9. Gilliver, K. The Inhibitory Action of Antibiotics on Plant Pathogenic Bacteria and Fungi. *Ann. Bot. (Oxford, U. K.)* **1946,** *10* (39), 271-282.

10. Prabhakaran, P.; Kale, S. S.; Puranik, V. G.; Rajamohanan, P. R.; Chetina, O.; Howard, J. A. K.; Hofmann, H.-J.; Sanjayan, G. J. Sequence-Specific Unusual (1→2)-Type Helical Turns in α/β-Hybrid Peptides. *J. Am. Chem. Soc.* **2008,** *130* (52), 17743-17754.

11. Kheria, S.; Nair, R. V.; Kotmale, A. S.; Rajamohanan, P. R.; Sanjayan, G. J. The role of N-terminal proline in stabilizing the Ant-Pro zipper motif. *New J. Chem.* **2015,** *39* (5), 3327-3332.

12. Nair, R. V.; Kotmale, A. S.; Dhokale, S. A.; Gawade, R. L.; Puranik, V. G.; Rajamohanan, P. R.; Sanjayan, G. J. Formation of a pseudo-β-hairpin motif utilizing the Ant–Pro reverse turn: consequences of stereochemical reordering. *Org. Biomol. Chem.* **2014,** *12* (5), 774-782.

13. Ramesh, V. V.; Priya, G.; Kotmale, A. S.; Gonnade, R. G.; Rajamohanan, P. R.; Sanjayan, G. J. Multifaceted folding in a foldamer featuring highly cooperative folds. *Chem. Comm.* **2012,** *48* (91), 11205-11207.

14. Cameron, A. J.; Squire, C. J.; Edwards, P. J. B.; Harjes, E.; Sarojini, V. Crystal and NMR Structures of a Peptidomimetic β-turn which provides facile synthesis of 13-membered Cyclic Tetrapeptides. *Chem. Asian J.* **2017**, (accepted) DOI: 10.1002/asia.201701422.

15. DeZoysa, G. H.; Sarojini, V. A Feasibility Study Exploring the Potential of Novel Battacin Lipopeptides As Antimicrobial Coatings. *ACS Appl. Mater. Interfaces* **2017,** *9* (2), 1373-1383.

16. De Zoysa, G. H.; Cameron, A. J.; Hegde, V. V.; Raghothama, S.; Sarojini, V. Antimicrobial Peptides with Potential for Biofilm Eradication: Synthesis and Structure Activity Relationship Studies of Battacin Peptides. *J. Med. Chem.* **2015,** *58* (2), 625-639.

17. Qin, C.; Zhong, X.; Bu, X.; Ng, N. L. J.; Guo, Z. Dissociation of Antibacterial and Hemolytic Activities of an Amphipathic Peptide Antibiotic. *J. Med. Chem.* **2003,** *46* (23), 4830-4833.

18. Jin, L.; Bai, X.; Luan, N.; Yao, H.; Zhang, Z.; Liu, W.; Chen, Y.; Yan, X.; Rong, M.; Lai, R. A Designed Tryptophan-and Lysine/Arginine-Rich Antimicrobial Peptide with Therapeutic Potential for Clinical Antibiotic-Resistant *Candida albicans* Vaginitis. *J. Med. Chem.* **2016,** *59* (5), 1791-1799.

19. Kohli, R. M.; Walsh, C. T.; Burkart, M. D. Biomimetic synthesis and optimization of cyclic peptide antibiotics. *Nature* **2002,** *418* (6898), 658-661.

20. Xiao, Q.; Pei, D. High-Throughput Synthesis and Screening of Cyclic Peptide Antibiotics. *J. Med. Chem.* **2007,** *50* (13), 3132-3137.

21. Levitt, M. A simplified representation of protein conformations for rapid simulation of protein folding. *J. Mol. Biol.* **1976,** *104* (1), 59-107.

22. Chou, P. Y.; Fasman, G. D. β-turns in proteins. *J. Mol. Biol.* **1977,** *115* (2), 135-175.

23. Perczel, A.; McAllister, M. A.; Csaszar, P.; Csizmadia, I. G. Peptide models 6. New .beta.-turn conformations from ab initio calculations confirmed by x-ray data of proteins. *J. Am. Chem. Soc.* **1993,** *115* (11), 4849-4858.

24. Wang, C. K.; Northfield, S. E.; Colless, B.; Chaousis, S.; Hamernig, I.; Lohman, R.-J.; Nielsen, D. S.; Schroeder, C. I.; Liras, S.; Price, D. A.; Fairlie, D. P.; Craik, D. J. Rational design and synthesis of an orally bioavailable peptide guided by NMR amide temperature coefficients. *Proc. Natl. Acad. Sci. U S A.* **2014,** *111* (49), 17504-17509.

25. Cierpicki, T.; Otlewski, J. Amide proton temperature coefficients as hydrogen bond indicators in proteins. *J. Biomol. NMR* **2001,** *21* (3), 249-261.

26. Jois, D. S. S.; Vijayan, S. S. M.; Easwaran, K. R. K. NMR and X-ray crystallographic studies on cyclic tetrapeptide, cyclo (D-Phe-Pro-Sar-Gly). *Int. J. Pept. Protein Res.* **1996,** *48* (1), 12-20.

27. Tzagoloff, H.; Novick, R. Geometry of cell division in Staphylococcus aureus. *J. Bacteriol.* **1977,** *129* (1), 343-350.

28. Chung, C.-J.; Lin, H.-I.; Chou, C.-M.; Hsieh, P.-Y.; Hsiao, C.-H.; Shi, Z.-Y.; He, J.-L. Inactivation of Staphylococcus aureus and Escherichia coli under various light sources on photocatalytic titanium dioxide thin film. *Surf. Coat. Technol.* **2009,** *203* (8), 1081-1085.

29. Touhami, A.; Jericho, M. H.; Beveridge, T. J. Atomic force microscopy of cell growth and division in Staphylococcus aureus. *J. Bacteriol.* **2004,** *186* (11), 3286-3295.

30. Lv, Y.; Wang, J.; Gao, H.; Wang, Z.; Dong, N.; Ma, Q.; Shan, A. Antimicrobial Properties and Membrane-Active Mechanism of a Potential α-Helical Antimicrobial Derived from Cathelicidin PMAP-36. *PLoS ONE* **2014,** *9* (1), e86364.

31. Hartmann, M.; Berditsch, M.; Hawecker, J.; Ardakani, M. F.; Gerthsen, D.; Ulrich, A. S. Damage of the bacterial cell envelope by antimicrobial peptides gramicidin S and PGLa as revealed by transmission and scanning electron microscopy. *Antimicrob. Agents Chemother.* **2010,** *54* (8), 3132-3142.

32. Alkotaini, B.; Anuar, N.; Kadhum, A. A. H. Evaluation of Morphological Changes of Staphylococcus aureus and Escherichia coli Induced with the Antimicrobial Peptide AN5-1. *Appl. Biochem. Biotechnol.* **2015,** *175* (4), 1868-1878.

33. Munyuki, G.; Jackson, G. E.; Venter, G. A.; Kövér, K. E.; Szilágyi, L.; Rautenbach, M.; Spathelf, B. M.; Bhattacharya, B.; van der Spoel, D. β-Sheet Structures and Dimer Models of the Two Major Tyrocidines, Antimicrobial Peptides from *Bacillus aneurinolyticus*. *Biochemistry* **2013,** *52* (44), 7798-7806.

34. Chen, W. C.; Chou, D.-L.; Feingold, D. S. Dissociation Between Ion Permeability and the Lethal Action of Polyene Antibiotics on Candida albicans. *Antimicrob. Agents Chemother.* **1978,** *13* (6), 914-917.

35. Kagan, S.; Ickowicz, D.; Shmuel, M.; Altschuler, Y.; Sionov, E.; Pitusi, M.; Weiss, A.; Farber, S.; Domb, A. J.; Polacheck, I. Toxicity Mechanisms of Amphotericin B and Its Neutralization by Conjugation with Arabinogalactan. *Antimicrob. Agents Chemother.* **2012,** *56* (11), 5603-5611.

36. Vranken, W. F.; Boucher, W.; Stevens, T. J.; Fogh, R. H.; Pajon, A.; Llinas, M.; Ulrich, E. L.; Markley, J. L.; Ionides, J.; Laue, E. D. The CCPN data model for NMR spectroscopy: Development of a software pipeline. *Proteins: Struct., Funct., Genet.* **2005,** *59* (4), 687-696.

37. Krieger, E.; Koraimann, G.; Vriend, G. Increasing the precision of comparative models with YASARA NOVA—a self-parameterizing force field. *Proteins: Structure, Function, and Bioinformatics* **2002,** *47* (3), 393-402.

38. Harjes, E.; Harjes, S.; Wohlgemuth, S.; Müller, K.-H.; Krieger, E.; Herrmann, C.; Bayer, P. GTP-Ras Disrupts the Intramolecular Complex of C1 and RA Domains of Nore1. *Structure* **2006,** *14* (5), 881-888.

39. Karplus, M. Vicinal Proton Coupling in Nuclear Magnetic Resonance. *Journal of the American Chemical Society* **1963,** *85* (18), 2870-2871.

40. Pardi, A.; Billeter, M.; Wüthrich, K. Calibration of the angular dependence of the amide proton-Cα proton coupling constants, 3JHNα, in a globular protein: Use of 3JHNα for identification of helical secondary structure. *J. Mol. Biol.* **1984,** *180* (3), 741-751.

41. Wiegand, I.; Hilpert, K.; Hancock, R. E. W. Agar and broth dilution methods to determine the minimal inhibitory concentration (MIC) of antimicrobial substances. *Nat. Protoc.* **2008,** *3* (2), 163-175.

42. Reference Method for Broth Dilution Antifungal Susceptibility Testing of Yeasts; Approved Standard. In *CLSI document M27-A*, Wayne: Clinical and Laboratory Standards Institute: 1997.

Table of Contents Graphic